

# Influence of the impurity content on the density and viscosity of olive oily fluids

 P. Vallesquino-Laguna<sup>a,✉</sup> and  A. Tirado-Esquinas<sup>a</sup>

<sup>a</sup>Department of Bromatology and Food Technology. ETSIAM – University of Córdoba. Campus de Rabanales s/n, 14080, Córdoba (Spain).

<sup>✉</sup>Correspondence: [bt1valap@uco](mailto:bt1valap@uco)

*Submitted: 12 May 2023; Accepted: 11 July 2023; Published online: 26 December 2023*

**SUMMARY:** In this work, as a case study, the measurement of the density ( $\rho$ ) and the dynamic viscosity ( $\mu$ ) of 12 different fluids (taken from a conventional oil mill) has been carried out. The variability of the samples processed shows that their impurity contents  $c$  (between 0.5–5.87%), together with the temperature  $t$  (which varied between 20–30 °C), can affect the values of  $\rho$  and  $\mu$ . However, this variation has been shown to be different depending on the case, being of the order of 1% for density or even more than 50% for dynamic viscosity. The fact that  $\mu$  can be sensitive to the presence of impurities opens up a line of study that could be used to estimate such impurity content, in real time, by means of relatively simple methods.

**KEYWORDS:** *Impurities; Mill; Olive Oil; Process; Temperature; Water*

**RESUMEN:** *Influencia del contenido de impurezas sobre la densidad y viscosidad de fluidos oleosos.* En este trabajo, como caso de estudio, se ha llevado a cabo la medida de la densidad ( $\rho$ ) y de la viscosidad dinámica ( $\mu$ ) de 12 fluidos diferentes tomados de una almazara convencional. La variabilidad de las muestras procesadas indica que el contenido de impurezas  $c$  (entre el 0,5%–5,87 %), junto con la temperatura  $t$  (que varió nominalmente entre 20 °C–30 °C), pueden afectar a los valores de  $\rho$  y  $\mu$ . Sin embargo, esta variación se ha mostrado diferente dependiendo del caso, siendo del orden del 1 % para la densidad o incluso mayor del 50% para la viscosidad dinámica. El hecho de que  $\mu$  pueda ser sensible a la presencia de impurezas abre una línea de estudio que podría ser aprovechada para estimar tal contenido de impurezas, en tiempo real, por medio de métodos relativamente sencillos.

**PALABRAS CLAVE:** *Aceite de Oliva; Agua; Almazara; Impurezas; Proceso; Temperatura*

**Citation/Cómo citar este artículo:** Vallesquino-Laguna P, Tirado-Esquinas A. 2023. Influence of the impurity content on the density and viscosity of olive oily fluids. *Grasas Aceites* 74 (4), e533. <https://doi.org/10.3989/gya.0534231>

**Copyright:** ©2023 CSIC. This is an open-access article distributed under the terms of the Creative Commons Attribution 4.0 International (CC BY 4.0) License.

## 1. INTRODUCTION

The production of olive oil requires a series of unit operations which, applied to the incoming raw olives, serve to obtain the final product. Focusing our attention on the intermediate and final stages of this process, it should be noted that the production fluids treated are usually accompanied by a series of undesirable impurities (Dammak *et al.*, 2015; Gila *et al.*, 2020) which must be separated from the main juice in order to obtain the desired EVOO (extra virgin olive oil). In this context, it is well-known (Hermoso *et al.*, 1996; Uceda *et al.*, 2006) that currently, after milling and malaxation, a first centrifugation is often applied (with a horizontal centrifuge, usually called ‘decanter’). The result of this operation is an oily phase which still contains remnants of vegetation water and other substances such as pulp, olive stones and even yeasts. In order to eliminate these substances, it is also common to carry out other subsequent operations which finally allow the production of the EVOO. These operations include sieving, a second centrifugation (with a vertical or ‘plate’ separator), filtering and natural decantation (these last two operations are not always performed in the order indicated).

Taking into account the set of unit operations mentioned above, it is clear that, for their management, it may be of interest to know beforehand, among many other factors, the physical properties of the oily fluids treated in the final stages of the process, since this knowledge could help to improve the yield and quality of the final product (Hermoso *et al.*, 1996; Alba, 2008). In this sense, it is noteworthy that there are several works that have addressed the study of properties such as the density and the viscosity of olive oil and its fatty acids (Cedeño *et al.*, 1999; Bonnet *et al.*, 2011; Nierat *et al.*, 2013; Gila, 2017), paying special attention to the variations that these properties can undergo with temperature changes. In other works, the focus has been mainly on the search for robust models which could allow the estimation of such properties with different types of oils, including olive oil (Herschel, 1922; Fasina *et al.*, 2006; Giap, 2010; Esteban *et al.*, 2012; Sahasrabudhe *et al.*, 2017). However, the presence of impurities and their influence on these parameters is an area of study that perhaps has not yet received enough attention (Gila, 2017), despite the fact that these substances can affect the quality and preservation of the EVOO, which may ultimately have a negative impact on its price.

In the above context, this work is presented to treat (as a case study) the determination of the density ( $\rho$ ) and the dynamic viscosity ( $\mu$ ), at different temperatures, of various oily fluids taken at different production stages, and campaign dates, from a conventional oil mill. To this end, the content of impurities ( $c$ ) present in these production fluids (non-final products) will be evaluated, and an attempt will be made to relate this content to the density and viscosity variations observed. Likewise, the Newtonian nature of these intermediary products will also be analyzed to verify whether the impurities present in them could cause any change in this respect. This analysis will be made by means of inexpensive devices that were designed and built in a laboratory. In addition, the effort developed in this work will try to elucidate whether the content of impurities, present in any oily fluid, could be estimated by simpler and faster methods than those currently used, which could be of interest for future applications.

## 2. MATERIALS AND METHODS

### 2.1. Test samples

In this work, 12 oily samples (approximately 10 l each) were collected between December 2019 and February 2020 from an olive oil mill (‘almazara’) located near Priego de Córdoba (Córdoba, Spain). Each of these samples had different characteristics and appearance (see Figure 1), mainly due to the date of collection and the point chosen for sampling. In summary, Table 1 shows some data of interest related to these samples. At this point, it should be noted that the production process carried out by the aforementioned ‘almazara’ was based on a ‘continuous conventional system’. In this system, each processing line uses (after cleaning, washing, milling and kneading) a two-way centrifugal decanter (‘horizontal centrifuge’) for solid-liquid separation, and a disc stack centrifuge (‘vertical centrifuge’) for liquid-liquid separation (Uceda *et al.*, 2006). In addition, the oil must not be filtered, but it can be sieved after the decanter step and can be clarified (with dynamic settling tanks) after the vertical centrifuge.

### 2.2. Lab equipment

In order to conduct the necessary experiments, it was decided to build several tube viscometers (Steffe, 1996), whose geometry is described in Figure 2.

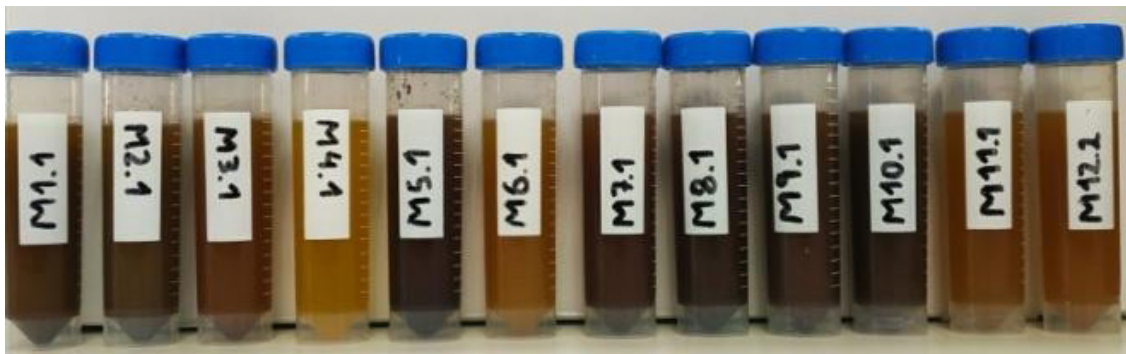


FIGURE 1. Appearance of some sub-samples taken from the oily fluids available.

TABLE 1. Sampling date, sampling point and origin (source) of the test samples

Sample	Sampling Date	Sampling Point - Source
M1	Dec 10th 2019	Sieve after Decanter – tree olives
M2	Dec 10th 2019	Sieve after Decanter – tree olives
M3	Jan 14th 2020	Sieve after Decanter – tree olives
M4	Jan 14th 2020	Vertical Centrifuge – tree olives
M5	Jan 30th 2020	Decanter directly – tree olives
M6	Jan 30th 2020	Vertical Centrifuge – tree olives
M7	Jan 30th 2020	Sieve after Decanter – tree and ground olives
M8	Jan 30th 2020	Sieve after Decanter – tree olives
M9	Feb 11th 2020	Sieve after Decanter – tree olives
M10	Feb 11th 2020	Sieve after Decanter – ground olives
M11	Feb 11th 2020	Sieve after Decanter – tree olives
M12	Feb 11th 2020	Vertical Centrifuge – tree olives

For manufacturing each viscometer, a calibrated plastic vessel was mainly required (to contain the fluid to be tested), as well as a transparent polyethylene tube (whose length and diameter were fixed by design to facilitate the development of laminar flow through the duct). The vessel utilized in each device had a capacity of one liter and it was marked with different reference lines to measure the fluid heads ( $h$ ) reached inside it. The tube length ( $L$ ) and the diameter ( $D$ ), selected to construct the viscometers, followed these combinations to modulate different flow rates, shear rates or shear stresses throughout the experiments:  $L=0.2$  m,  $D=4.07$  mm;  $L=0.4$  m,  $D=4.07$  mm;  $L=1$  m,  $D=7.63$  mm;  $L=1,20$  m,  $D=3.87$  mm and  $L=1.60$  m,  $D=4.10$  mm. The tube insertion length ( $\delta$ ) inside the vessel (see Figure 2) was 0.01 m in all cases.

In addition to the above, other auxiliary materials were needed to run the tests: two glass thermometers (to determine the fluid temperature at the viscometer pipe ends) with a measuring range of  $-10$  °C to  $+60$  °C and with an accuracy of  $\pm 1$  °C; six laboratory

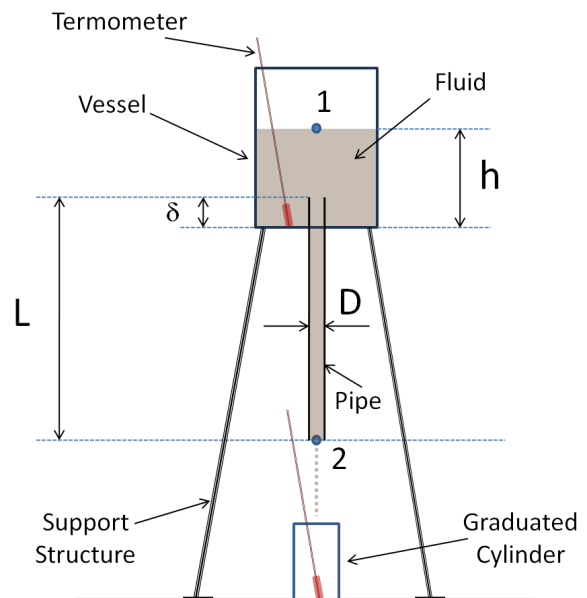


FIGURE 2. Scheme of a tube viscometer used in this study.

graduated cylinders of 100 ml (with an accuracy of  $\pm 1$  ml), and five more of 250 ml (with an accuracy of  $\pm 2$  ml), to collect the volumes that would be use-

ful for determining densities and flow rates; two laboratory scales with accuracies of  $\pm 0.01$  g and  $\pm 0.001$  g, respectively; a digital chronometer (with a resolution of 0.01 s); A centrifuge with adjustable temperature and speed controls (suitable for 50 ml test tubes from  $-9$  °C to  $+40$  °C, and from 200 rpm to 14000 rpm, respectively); two refrigerating chambers (at  $4.5$  °C and  $12$  °C) and a freezing chamber (at  $-18$  °C) for storing samples during testing; ice blocks, hot water and 10-l buckets for rapid cooling (or heating) of oily samples by indirect contact; auxiliary bottles of 1.5 l to contain samples if required; calibrated 50-ml tubes for centrifugal separation; pipettes and syringes for handling or transferring samples; a measuring tape (calibrated in millimetres) and various office supplies (scissors, adhesive tape, markers, etc.).

### 2.3. Viscosity and density tests of oily samples

The experiments in this section were performed using a viscometer with a tube length ( $L$ ) of 0.4 m and a diameter ( $D$ ) of 4.07 mm. Having made the above clarification, it should be noted that the original samples (see section 2.1 and Table 1) were first homogenized by manual shaking and then divided into different 1.5-l auxiliary bottles to facilitate the tasks involved in the tests. The bottles were kept cold (at  $4.5$  °C or  $-18$  °C, depending on the expected time before use) to avoid any microbiological activity (such as fermentation due to the presence of yeasts).

When it was convenient, one of the refrigerated bottles (at  $4.5$  °C) was taken and tempered in the laboratory (at  $23$  °C) for (1 – 2) h. Bearing in mind that the fluid temperature in the tests had to be similar to that present in the industrial production of olive oil (of the order of  $20$  °C –  $30$  °C), each viscosity experiment was started when the sample temperature was approaching  $20$  °C. At that moment, the fluid was poured into the viscometer vessel (which was exposed to the atmosphere) and, after its stabilization and its flow through the tube, it was collected for a given time in a lab cylinder (placed in the lower part of the experimental setup, see Figure 2). Fluid volume ( $V$ ), stored in the graduated cylinder, was also weighed with a laboratory scale to estimate its density  $\rho$ , (Eq. 1)

$$\rho = \frac{m}{V} \quad (\text{Eq. 1})$$

where  $m$  was the mass linked to  $V$ .

In addition, flow rate  $Q$  was estimated from  $V$  taking into account the time  $\tau$  needed to collect such fluid volume (Eq. 2)

$$Q = \frac{V}{\tau} \quad (\text{Eq. 2})$$

On the other hand, the fluid temperature was measured at two points (at the input and output ends of the viscometer pipe), and adjusted by indirect contact using hot or cold water before the fluid was poured into the viscometer vessel. The fluid height  $h$  inside the vessel (see Figure 2) was observed at the beginning and at the end of each test, and the mean of these measurements was taken as a representative value (usually in the range of 4 – 6 cm).

From the procedure described above, which was applied 144 times (12 tests, in the range of  $20$  °C –  $30$  °C, for each of the 12 types of fluid treated), and taking into account what it is described in section 2.2, the values for dynamic viscosity  $\mu$  were estimated from the following expression (Eq. 3), based on the Hagen-Poiseuille equation and on the energy equation (Singh and Heldman, 2009).

$$\mu = \frac{\Delta p \pi D^4}{128 L Q} = \frac{\rho g (h + L - \delta) \pi D^4}{128 L Q} \quad (\text{Eq. 3})$$

where  $\Delta p = \rho g (h + L - \delta)$  is the pressure loss between 1 and 2 (see Figure 2),  $g$  is the gravitational acceleration, and the other variables are those just indicated in this section and in paragraph 2.2. The use of Eq. 3, to estimate  $\mu$  requires, in principle, the assumptions that the fluid tested is Newtonian, the kinetic heads are negligible and the flow is stationary and perfectly laminar throughout the entire length  $L$ . This last assumption implies that the effect of the inlet length and the local head losses at the pipe inlet can also be neglected. The accuracy of the previous approximations was analyzed for flows such as those treated here in Tirado (2020), where it was verified that for oily fluids at very low Reynolds numbers (of the order or less than 10) such premises could be accepted. To minimise possible errors, it should also be noted that the values of  $\rho$  employed in Eq. 3, were obtained, in each case, from polynomial interpolation taking 12 pair of values ( $t, \rho$ ) available as reference for each type of fluid from the experiments.

## 2.4. Impurity content tests

Considering as impurities, as a whole, all those remains of vegetation water, pulp, olive stone (and even yeasts) present in the EVOO, in this work this matter content was determined according to an alternative method (Vallesquino and Tirado, 2023), different from the official one (IOC, 2019), in order to obtain sufficiently accurate results while simplifying the experimental procedure. Therefore, the impurity content  $c$ , expressed as a percentage of the volume of impurities ( $V_{imp}$ ) and the sample volume ( $V_{sp}$ ) (Eq. 4):

$$c (\%) = \frac{V_{imp}}{V_{sp}} 100 \quad (\text{Eq. 4})$$

could be estimated as follows: firstly, two samples (of around 40 ml) were taken from every type of fluid previously treated in the ‘viscosity and density tests of oily samples’ (see section 2.3), and they were poured into two centrifuge tubes like those shown in Figure 1. These tubes were allowed to decant naturally in the laboratory, between (24 – 48) h at 23 °C, and then centrifuged at 3900 rpm for 12 min at 27 °C. After that, the volume of impurities present in each sample was clearly visible (see the lower part of each tube in Figure 3, as an example), and this volume (in many cases very small) could be determined by applying the appropriate operations (Vallesquino and Tirado, 2023).

The bulk density of the impurities was determined separately, with the aim of estimating a more representative value than that which could be obtained from sub-samples like those shown in Figure 3. With this in mind, and depending on the content

of non-oily remains, among 2 – 4 samples of each type of fluid were randomly selected (from those collected in 1.5-l bottles, as described in section 2.3), and the impurities present in their bottoms were extracted. Such sediments were formed by gravitational decantation until an effective separation between the substances could be visually verified. This task could take no less than (2–3) wk per sample, applying temperatures between 4.5 – 23 °C to avoid unwanted fermentations. Next, the bottom content extracted from these samples was homogenized and 50 ml were poured into one or two centrifuge tubes (depending on the amount of impurities available) and centrifuged at 3900 rpm for 12 min at 27 °C. Once this operation had been carried out, the appearance of the samples obtained was similar to that shown in Figure 3, but with a more abundant impurity phase (of the order of 30 ml), in which it was generally possible to observe vegetation water (about 55%) and insoluble solids (about 45%). The bulk density of each impurity sample could then be estimated by a simple fraction between the mass and the volume of the impurities (after carefully removing the residual oil that could be present in each tube).

## 2.5. Rheological tests of oily samples

These experiments were designed to verify whether the dynamic behavior of the fluids studied in this work was in accordance with Newton’s law of viscosity. Therefore, the relationship between  $\sigma_w$  (wall shear stress of the flow) and  $\left(\frac{du}{dr}\right)_w$  (wall shear rate) was analyzed. According to Steffe (1996),  $\sigma_w$  can be expressed as follows (Eq. 5) for the laminar flow of a time-independent fluid through a cylindrical tube (Figure 2):

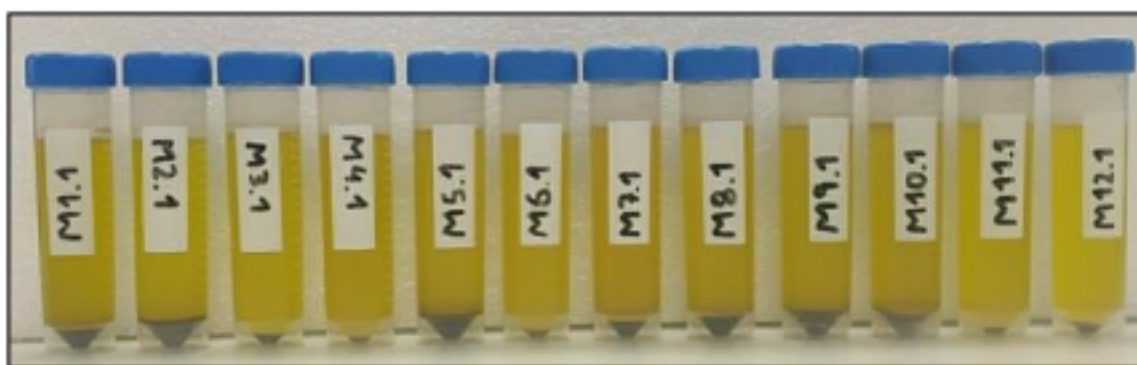


FIGURE 3. Appearance of the sub-samples shown in Figure 1 after 24 h of natural decantation and further centrifugation at 3900 rpm for 12 min at 27 °C.

$$\sigma_w = \frac{\rho g(h + L - \delta)D}{4L} \quad (\text{Eq. 5})$$

For its part, the shear rate  $\left(\frac{du}{dr}\right)_w$  depends on the fluid treated. However, this variable could be expressed as a function 'f[ ]' of this elemental ratio ( $\gamma_e$ ) (Eq. 6):

$$\left(\frac{du}{dr}\right)_w = f\left[\frac{32Q}{\pi D^3}\right] = f[\gamma_e] \quad (\text{Eq. 6})$$

which can be used in further analysis.

Considering the above premises (together with the available resources), and trying to obtain an adequate set of pairs ( $\gamma_e$ ,  $\sigma_w$ ), it was considered appropriate to use four of the viscometers already mentioned in section 2.2 in these tests. The dimensions of these devices were:  $L = 0.2$  m,  $D = 4.07$  mm;  $L = 1$  m,  $D = 7.63$  mm;  $L = 1.20$  m,  $D = 3.87$  mm and  $L = 1.60$  m,  $D = 4.10$  mm. In addition, four samples were tested with each of these viscometers: M1, M4, M7 and M10, chosen because they showed a representative variability in impurity content. In order to avoid unwanted fermentations (due to the racking, aeration and duration of these tests), about 3 l of each of these samples were pasteurized (at 80 °C for 45 min). They were then cooled (at a temperature close to 23 °C) and analyzed 5 times with each of the viscometers cited above, following a procedure analogous to that described in section 2.3. Furthermore, it should be noted that the data previously obtained from the unpasteurized samples (according to section 2.3) were used as control data for the corresponding comparisons.

### 3. RESULTS AND DISCUSSION

#### 3.1. Impurity density and content

Table 2 shows the data related to the impurity content  $c$ , as well as the bulk density values ( $\rho_{ap}$ ) linked to them. From these data, it is worth noting that the minimum and maximum  $c$  values are of the order of 0.5% (sample M4) and 5.87% (sample M2), respectively. These data can be considered normal when compared to those obtained by other authors (Hermoso *et al.* 1996; Uceda *et al.* 2006; Bejaoui *et al.*, 2013; Dammak *et al.*, 2015; Gila, 2017), who presented  $c$  results which varied from 1 to 15% for fluids taken from the decanter, and from 0.2 – 0.6%

TABLE 2. Impurity content  $c$  (%) and impurity bulk density ( $\rho_{ap}$ ) of the samples treated.

Sample and Date	$c$ (%)	$\rho_{ap}$ (kg / m <sup>3</sup> )
M1 - Dec 10 <sup>th</sup> 2019	3.61 ± 0.11	1240 ± 8.2
M2 - Dec 10 <sup>th</sup> 2019	5.87 ± 0.33	1167 ± 10.3
M3 - Jan 14 <sup>th</sup> 2020	1.13 ± 0.13	1196 ± 7.5
M4 - Jan 14 <sup>th</sup> 2020	0.50 ± 0.12	1108
M5 - Jan 30 <sup>th</sup> 2020	5.00 ± 0.18	1171 ± 12.5
M6 - Jan 30 <sup>th</sup> 2020	1.14 ± 0.14	1089 ± 5.7
M7 - Jan 30 <sup>th</sup> 2020	2.00 ± 0.20	1146 ± 9.1
M8 - Jan 30 <sup>th</sup> 2020	4.05 ± 0.20	1168 ± 6.5
M9 - Feb 11 <sup>th</sup> 2020	4.50 ± 0.24	1135 ± 9.7
M10 - Feb 11 <sup>th</sup> 2020	5.38 ± 0.50	1080 ± 11.0
M11 - Feb 11 <sup>th</sup> 2020	0.89 ± 0.14	1218
M12 - Feb 11 <sup>th</sup> 2020	1.27 ± 0.05	1126 ± 5.2

The values shown are the mean ± SD of two replicates (for samples M4 and M11  $\rho_{ap}$  a single test was done in due to the impurity content available).

(Bejaoui *et al.*, 2013; Dammak *et al.*, 2015) for samples collected from the vertical centrifuge (note that samples M4, M6 and M12 came from the vertical centrifuge, and the other ones from the horizontal decanter; see Table 1). The factors causing this variability (in this study and in those cited) can be diverse and they could have their roots in agronomic and technological aspects (Hermoso *et al.*, 1996; Uceda *et al.*, 2006; Vallesquino and Tirado, 2023). Most likely, in the absence of more data, the lower  $c$  results (for the samples taken from the decanter in this study) could be related to longer residence times, higher processing temperatures and smaller outlet radii for the oily phase. In this context, sample M11 could be a representative example of these operating conditions, as it appears to have been taken from a vertical centrifuge, but was actually collected from a decanter.

Regarding the bulk density values ( $\rho_{ap}$ ) presented in Table 2, it is noteworthy that they all fell within a range of 1080 kg/m<sup>3</sup> – 1240 kg/m<sup>3</sup>. Attempting to compare these data with those of other studies, it is notorious that Gila (2017) points out that there are few references on this issue in the literature, placing  $\rho_{ap}$  (through simulations) in a range of 1025 kg/m<sup>3</sup> to 1225 kg/m<sup>3</sup>. In Alba (2008), the density of oily wastewaters (*alpechines*) is set around 1050 kg/m<sup>3</sup>, and that of the pomace at 1200 kg/m<sup>3</sup> (values compatible with those presented here).

It is also remarkable that  $\rho_{ap}$  seems to be smaller for the samples taken from the vertical centrifuge

(M4, M6 and M12) compared to those obtained from the decanter. This could make sense if one considers that, according to Stokes's law (Mafart and Béliard, 1994), the densest and largest particles are easier to separate from the liquid phase in the first centrifugation (with the decanter). Similarly, although the number of data available is not large, the values for  $\rho_{ap}$  in Table 2 seem to show a decreasing trend as the production campaign progresses. This could be related to the changing nature of the raw material (maturity stage) and could be analyzed from a greater number of samples in future works.

### 3.2. Rheological tests results

Figure 4 shows the data of the shear stress  $\sigma_w$  (see Eq. 5), as a function of the elemental ratio  $\gamma_e = \frac{32Q}{\pi D^3}$ , obtained from the rheological tests developed according to section 2.5 (at laboratory temperature of 23 °C). The fluids treated in these experiments were: M1, M4, M7 and M10. It can be seen in Figure 4 that the relationship between  $\sigma_w$  and  $\gamma_e$  is linear, with zero ordinate at the origin. According to Steffe (1996), the data presented do not agree well with the Bingham or power law models, but they do with that expected for a Newtonian fluid. In such a case (Newtonian fluid), it could be stated directly (Eq. 7):

$$\left(\frac{du}{dr}\right)_w = \gamma_e = \frac{32Q}{\pi D^3} \quad (\text{Eq. 7})$$

$$\sigma_w = \mu \left(\frac{du}{dr}\right)_w \quad (\text{Eq. 8})$$

which implies that the shear rate  $\left(\frac{du}{dr}\right)_w$  is directly equal to  $\gamma_e = \frac{32Q}{\pi D^3}$ , and that the slope of the function  $\left(\frac{du}{dr}\right)_w = f[\gamma_e]$  (see also Eq. (6)) corresponds to the dynamic viscosity ( $\mu$ ) of the fluids tested. In this scenario, it so happens that these fluids would have a  $\mu$  value (at 23 °C) that could be of the order of 0.07 Pa·s (sample M4) or 0.074 Pa·s (sample M10).

Other authors, like Fasina *et al.* (2006), Bonnet *et al.* (2011) or Gila (2017), have also found that olive oil (without impurities) shows a Newtonian behavior, reporting values for  $\mu$  which are similar to those indicated here. This circumstance confirms that the moderate presence of impurities does not seem to affect the Newtonian nature of olive oil. On the other hand, it is worth noting that the pasteurization

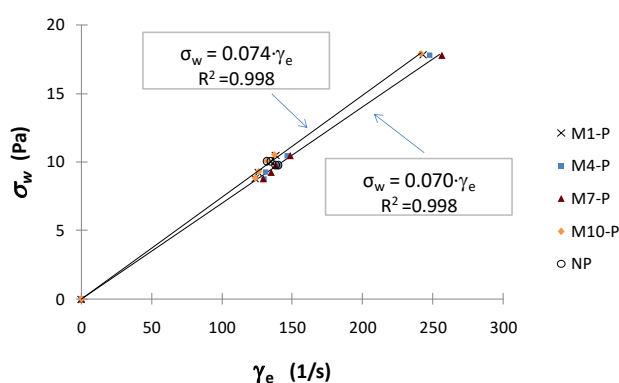


FIGURE 4. Relationship between  $\gamma_e$  (shear rate) and  $\sigma_w$  (shear stress) for some samples (M1, M4, M7 and M10) after pasteurization (-P) and without pasteurization ('O' symbol).

Each pair of values ( $\gamma_e$ ,  $\sigma_w$ ) was obtained for  $t = 23$  °C by polynomial interpolation from 5 replicates made at temperatures between (20 – 25) °C. The experimental error expected is of the order of 4.2%.

treatment does not seem to have any effect on the rheological behavior of the fluids analyzed, since the control samples (without heat treatment, see section 2.3) have values for  $\mu$  that are equivalent to those of the pasteurized samples. This aspect can be observed in Figure 4, where the values for M1, M4, M7 and M10 (marked with 'O' symbol and taken from the control samples) are perfectly in line with the rest of the values (obtained from pasteurized samples).

Besides the former, the data presented in Figure 4 are not evenly distributed. This effect is due to the design of the viscometers used, which conditions the values for  $\gamma_e$  that they can present. For instance, in those viscometers with  $D \approx 4$  mm,  $\gamma_e$  was in the range of 120 – 150 s<sup>-1</sup>, and the remaining  $\gamma_e$  values were related to the device with  $D = 7.63$  mm (including the singular point (0,0), explained by the fact that no fluid could be retained at the bottom end of the viscometer tube when it was finally emptied). Considering the results obtained in this study, it could be recommended for future works to follow an experimental design slightly different from the one treated here. In this regard, a better approach could be implemented by using a set of tube viscometers with a greater variety of tube diameters and fewer length options. Nevertheless, the results shown in Figure 4 could be useful references for the olive oil industry, since  $\gamma_e$  (see Eq. 7) is usually less than 250 s<sup>-1</sup> for oily flows of (1000 – 2000) l/h flowing through (3–5) cm diameter tubes (common operating values associated with decanters or vertical centrifuges).

### 3.3. Density and viscosity of the oily samples

Figure 5 presents the density values ( $\rho$ ) for all the samples tested. On the left side of this Figure,  $\rho$  is plotted as a function of the impurity content  $c$  (see Eq. 4), taken as reference, as a first approximation, only three temperature values ( $t = 20\text{ }^\circ\text{C}$ ,  $t = 25\text{ }^\circ\text{C}$  and  $t = 30\text{ }^\circ\text{C}$ ) to carry out a simpler analysis. On the right side of Figure 5,  $\rho$  is shown according to the model results which will be presented later.

Observing the relationship between  $\rho$ ,  $c$ , and  $t$  in the cited Figure, it is clear (despite the scatter) that the density showed a linear increasing trend as the impurity content increased. However,  $\rho$  tended to decrease as temperature  $t$  increased (at  $30\text{ }^\circ\text{C}$  the values for  $\rho$  were, in general, smaller than at  $25$  or  $20\text{ }^\circ\text{C}$ ). Likewise, the gap (separation) between the functions  $\rho = f(c)$  maintained a certain linearity (the ordinate at the origin and the slope of such functions grew linearly with  $t$ ), which suggests that the general relationship between  $\rho$ ,  $c$  and  $t$  could be of the form:

$$\rho = (a_1c + a_2)(a_3t + a_4) \quad (\text{Eq. 9})$$

where  $a_1$ ,  $a_2$ ,  $a_3$  and  $a_4$  are fitting parameters. In the scientific literature, the density of different types of oils, including olive oil, is usually adjusted by means of linear functions that depend on temperature (Esteban *et al.*, 2012; Gila, 2017). In addition, their resulting values are similar to those presented here, taking into account that the oils treated in this study contained impurities. Considering the above,  $\rho$  data were fitted to Eq. (9) as follows:

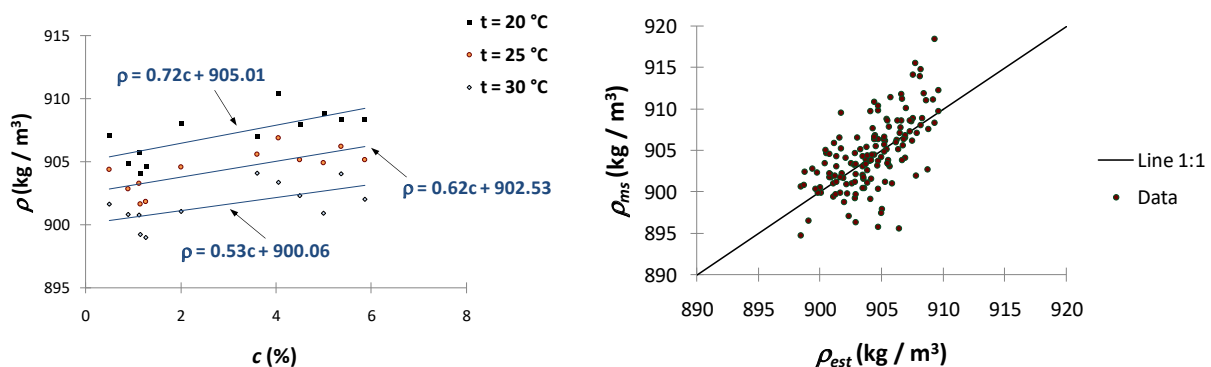


FIGURE 5. Relationship between the impurity content ( $c$ ) and the density of oily fluids ( $\rho$ ), at  $t$  temperatures of 20, 25 and  $30\text{ }^\circ\text{C}$  (left side), and comparison between the estimated density ( $\rho_{est}$ ) and the measured density ( $\rho_{ms}$ ) from the experiments (right side).

Each  $\rho$  value, on the left side, was obtained by polynomial interpolation (at constant impurity content  $c$ ) from 12 replicates made at different temperatures between ( $20 - 30$ )  $^\circ\text{C}$ . On the right side, each value for  $\rho$  was obtained from a single test, with  $R^2 = 0.402$  and  $(\text{RMS})^{0.5} = 3.327\text{ kg/m}^3$ .

$$\rho = (0.957c + 1.423 \cdot 10^3)(-4.030 \cdot 10^{-4}t + 0.644) \quad (\text{Eq. 10})$$

where the determination coefficient ( $R^2$ ) was equivalent to 0.402 and the residual mean square error (RMS) was of the order of  $11.070\text{ (kg/m}^3)^2$ .

Figure 5 (right side) presents the fluid density values  $\rho_{est}$  estimated from Eq. (10), in comparison to those measured in the experiments ( $\rho_{ms}$ ). Except for the scale factor of this Figure, which in this case tends to exaggerate the magnitude of the deviations, the main trend established by Eq. (10) is in agreement with the experimental data. Moreover, Figure 5 shows that, in order to accurately take into account the effect of the impurity content on  $\rho$ , it is necessary to measure the fluid density with a lower tolerance (of the order of 0.1%), since the density variations are not very sensitive to changes in  $c$  values. In this respect, it should be noted that the data scatter shown in this Figure is the result of possible errors associated with the measurement of volumes using the materials mentioned in section 2.2. These errors are unlikely to be greater than  $\pm 1.5\%$ , but they are sufficient to produce a maximum deviation of  $\pm 14\text{ kg/m}^3$ , which is compatible with the RMS value just indicated.

Regarding the dynamic viscosity ( $\mu$ ), Figure 6 presents the values of  $\mu$  in a similar way to that already performed with  $\rho$ . On the left side of such a Figure, three reference  $t$  values have been taken to analyze the variation in  $\mu$  with respect to the impurity content  $c$ . It is observed, as in the case of  $\rho$ , that

$\mu$  follows a linearly increasing trend with  $c$ , and a decreasing one (but not linear) with respect to  $t$ . On this occasion, the intercept and the slope of the fitting functions  $\mu = f(c)$  do not vary linearly with  $t$ , which leads to the assumption that the possible relationship between  $\mu$ ,  $c$  and  $t$  could be of the type:

$$\mu = (b_1 c + b_2) \left( \frac{b_3}{t} + b_4 \right) \quad (\text{Eq. 11})$$

$$\mu = (b_1 c + b_2) \left( \frac{b_3}{t^2} + \frac{b_4}{t} + b_5 \right) \quad (\text{Eq. 12})$$

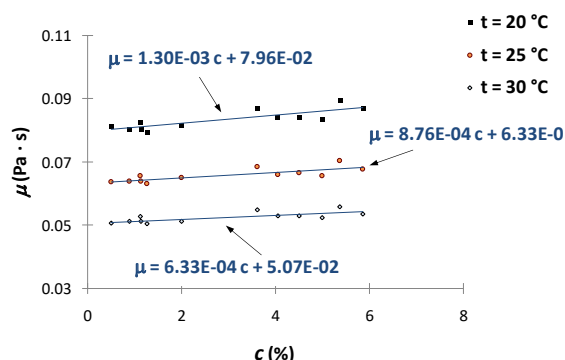
where  $b_1, b_2, b_3, b_4$  and  $b_5$  are fitting parameters.

According to several authors (Fasina *et al.* 2006; Esteban *et al.*, 2012; Gila, 2017; Sahasrabudhe *et al.*, 2017), the viscosity of diverse oils (including olive oil) could be estimated from different models which, essentially, are based on the Arrhenius equation:

$$\mu = A e^{\left(\frac{E_a}{RT}\right)} \quad (\text{Eq. 13})$$

where  $A$  is an empirical parameter,  $E_a$  is the activation energy,  $R$  is the universal gas constant, and  $T$  is the absolute temperature. Taking into account the exponential nature of the previous model, and the development of Taylor's series for any exponential function (Spiegel and Ribero, 1970):

$$e^x = 1 + x + \frac{x^2}{2!} + \frac{x^3}{3!} + \dots \quad (\text{Eq. 14})$$



it is obvious that Eq. (13) could be reformulated as a function such as:

$$\mu = d_1 + \frac{d_2}{T} + \frac{d_3}{T^2} + \dots \quad (\text{Eq. 15})$$

which is directly related to the Slotte's equation (Herschel, 1922). Note that, again,  $d_1, d_2, d_3, \dots$  are fitting parameters. For short temperature ranges (as occur in this study), where the slope of the function  $\mu = f(T)$  does not change excessively with temperature, it may be feasible to apply an expression like Eq. (15) by only using, as an approximation, two or three equation terms. Furthermore, if  $T$  is well above 273 K, Eq. (15) could even be adapted for Celsius degrees, achieving quite reasonable results (Vallesquino and Sánchez, 2023). Bearing in mind the above,  $\mu$  data were adjusted for two models, such as those shown in Eqs. (11) and (12), in which the Celsius scale was used in the first one (Eq. 16) and the Kelvin scale was applied in the second one (Eq. 17):

$$\mu = (-1.437 \cdot 10^{-3} c - 0.094) \left( \frac{-18.403}{t} + 0.073 \right) \quad (\text{Eq. 16})$$

$$R^2 = 0.982; \quad \text{RMS} = 3.252 \cdot 10^{-6} \text{ (Pa}\cdot\text{s)}^2$$

$$\mu = (4.672 \cdot 10^{-2} c + 3.087) \left( \frac{1.794 \cdot 10^5}{T^2} - \frac{1.118 \cdot 10^3}{T} + 1.751 \right) \quad (\text{Eq. 17})$$

$$R^2 = 0.987; \quad \text{RMS} = 2.351 \cdot 10^{-6} \text{ (Pa}\cdot\text{s)}^2$$

On the right side of Figure 6, the values for dynamic viscosity estimated by means of Eq. (17)

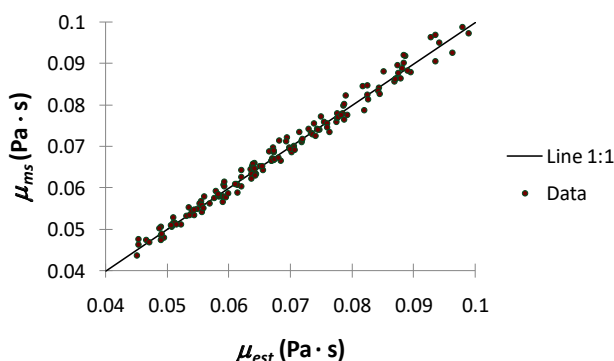


**FIGURE 6.** Relationship between the impurity content ( $c$ ) and the dynamic viscosity ( $\mu$ ), at  $t$  temperatures of 20, 25 and 30 (left side), and comparison between the estimated viscosity ( $\mu_{est}$ ) and the measured viscosity ( $\mu_{ms}$ ) from the experiments (right side).

Each  $\mu$  value, on the left side, was obtained by polynomial interpolation (at constant impurity content  $c$ ) from 12 replicates made at different temperatures between (20 – 30) °C. On the right side, each value of  $\mu$  was obtained from a single test, with  $R^2 = 0.987$  and  $(\text{RMS})^{0.5} = 1.533 \cdot 10^{-3} \text{ Pa}\cdot\text{s}$ .

( $\mu_{est}$ ) are plotted against those obtained from the experiments ( $\mu_{ms}$ ). It should be noted that, for the sake of clarity, the data related to Eq. 16 are not displayed in the Figure because they would overlap with those estimated from Eq. 17, (as can be inferred from  $R^2$  and RMS values associated to these equations).

On the other hand, it is also remarkable that the fitting accuracy of Eqs. 16 and 17 is higher than that of Eq. 10, (see also the right side of Figures 5 and 6). This fact reveals that the dynamic viscosity of olive oil is a variable that is sensitive to variations in temperature (this is well-known), but it is sensitive, as well, to variations in the impurity content. This aspect is relevant because, similar to the approach presented by Vallesquino and Sánchez (2023), by combining expressions such as those established in Eqs. 3 and 16 (or in Eqs. 3 and 17) it could be possible to calibrate empirical functions ( $\psi$ ) of the form:

$$c = \psi(\Delta p, Q, t, L, D) \quad (\text{Eq. 18.a})$$

$$\text{or } c = \psi(\Delta p, Q, T, L, D) \quad (\text{Eq. 18.b})$$

These  $\psi$  functions could, in the end, make it possible to estimate the impurity content  $c$  in real time (present in any oily must) if some simple sensors were installed on the production line. As an example, if Eqs. 3 and 16 were considered in this case, Eq. 18.a could be reformulated as:

$$c (\%) = \frac{\frac{\Delta P \pi D^4}{128 L Q}}{-1.437 \cdot 10^{-3} \left(-\frac{18.403}{t} + 0.073\right) - \frac{0.094}{1.437 \cdot 10^{-3}}} \quad (\text{Eq. 19})$$

where  $c$  is obtained, as a percentage, from two plant design parameters ( $L$  and  $D$ , in m) and three process line variables like  $Q$  (flow rate, in  $\text{m}^3/\text{s}$ ),  $t$  (temperature, in  $^\circ\text{C}$ ) and  $\Delta p$  (pressure drop, in Pa). Although Eq. (19) is only valid, as a rough approximation, for certain operating conditions (related to some samples taken from a determinate conventional olive oil mill), this approach opens the possibility of studying similar models that could be applied in any 'almazara', which could be of interest for the improvement of processes and products in the olive oil sector. In this regard, it should be pointed out that, in real manufacturing processes, knowledge of the

impurity content in oily fluids could help to make appropriate decisions on factors such as the residence time of the processed fluids in decanters (or in vertical centrifuges) and the choice of the most suitable type of clarification to be applied after the second centrifugation.

#### 4. CONCLUSIONS

As a case study, the density ( $\rho$ ) and the dynamic viscosity ( $\mu$ ) of 12 different oily fluids (taken from a conventional mill) have been measured, verifying the variability that these physical properties may present as a function of temperature ( $t$ ) and the impurity content ( $c$ ) of the samples treated.

In the case of  $\rho$ , its relationship with  $t$  and  $c$  has shown a linear trend, but this dependence is weak since large increases in temperature or impurity content are required for the density to vary significantly. In this work, it could serve as a reference that the density has experienced variations, of the order of less than 1%, when the temperature varied between 20–30  $^\circ\text{C}$  and the impurity content between 0.5–5.87 %.

Regarding dynamic viscosity, its dependence on  $t$  and  $c$  is of a different nature, as it can be quadratic for  $t$  and simply linear for  $c$ , in a context of Newtonian fluid behavior. The fact that the viscosity varies of the order of 50% or more, between 20–30  $^\circ\text{C}$  for a given value of  $c$ , allows one to confirm (as is usual for fluids) that  $\mu$  strongly depends on  $t$ . In the case of the relationship between  $\mu$  and  $c$  (for temperatures between 20–30  $^\circ\text{C}$ ), it is notable that the dependence of  $\mu$  on  $c$  is not so strong, but it is appreciable: when the impurity content varies from 0.5 to 5.87%, the dynamic viscosity of the oily fluids can reach variations of the order of 7–10% (much higher than that reported in the case of  $\rho$ ). In this scenario, the relationship between  $\mu$  and  $c$  could be used to determine the impurity content of a given oily fluid on line, (requiring only the implementation of some simple sensors on the process line), which could be used, ultimately, to improve the quality of the olive oil and its industrial process.

#### ACKNOWLEDGMENTS

The authors would like to thank invaluable help from the staff of 'S.C.A. Almazaras de la Subbética' for providing the samples used in this study. In the same way, they also would like to mention the De-

partment of Bromatology and Food Technology at the University of Córdoba, Spain, for funding, and the use of its facilities.

## REFERENCES

- Alba J, 2008. Elaboración del aceite de oliva virgen, in Barranco D (Ed.) *El cultivo del olivo*. Madrid, Spain, 657–697.
- Bejaoui MA, Gila A, Allouche, Y, Aguilera MP, Jiménez A, Beltrán G. 2013. Eficiencia de la clarificación del aceite de oliva virgen mediante decantación y centrifugación. *Actas del XVI Simposio Científico Técnico – Expoliva 2013 IND* – 36, 1–6.
- Bonnet JP, Devesvre L, Artaud J, Moulin, P. 2011. Dynamic viscosity of olive oil as a function of composition and temperature: A first approach. *Eur. J. Lipid Sci. Technol.* **113** (8), 1019–1025. <https://doi.org/10.1002/ejlt.201000363>
- Cedeño FO, Prieto MM, Bada JC, Alonso R. 1999. Estudio de la densidad y de la viscosidad de algunos ácidos grasos puros. *Grasas Aceites* **50** (5), 359–368. <https://doi.org/10.3989/gya.1999.v50.i5.680>
- Dammak I, Neves M, Souilem S, Isoda H, Sayadi S, Nakajima M. 2015. Material balance of olive components in virgin olive oil extraction processing. *Food Sci. Technol. Res.* **21** (2), 193–205. <https://doi.org/10.3136/fstr.21.193>
- Esteban B, Riba JR, Baquero G, Rius A, Puig R. 2012. Temperature dependence of density and viscosity of vegetable oils. *Biomass Bioener.* **42**, 164–171. <https://doi.org/10.1016/j.biombioe.2012.03.007>
- Fasina OO, Hallman H, Craig-Schmidt M, Clements C. 2006. Predicting temperature-dependence viscosity of vegetable oils from fatty acid composition. *J. Am. Oil Chem. Soc.* **83**, 899–903. <https://doi.org/10.1007/s11746-006-5044-8>
- Giap SGE. 2010. The hidden property of Arrhenius-type relationship: viscosity as a function of temperature. *J. Phys. Sci.* **21** (1), 29–39.
- Gila A. 2017. *Clarificación de los aceites de oliva vírgenes y su efecto en las características físico-químicas y sensoriales*. Doctoral dissertation. Universidad de Jaén, Spain.
- Gila A, Bejaoui MA, Beltrán G, Jiménez A. 2020. Rapid method based on computer vision to determine the moisture and insoluble impurities content in virgin olive oils. *Food Control* **113** (107210), 1–5. <https://doi.org/10.1016/j.foodcont.2020.107210>
- Hermoso M, González J, Uceda M, García-Ortiz A, Morales J, Frías L, Fernández A. 1996. *Elaboración de aceite de calidad. Obtención por el sistema de dos fases*. Consejería de Agricultura y Pesca - Junta de Andalucía. Sevilla, Spain.
- Herschel, WH. 1922. The change in viscosity of oils with the temperature. *Ind. Eng. Chem.* **14** (8), 715–722.
- IOC. 2019. Trade standard applicable to olive oils and olive-pomace oils. COI/T.15/NC No 3/ Rev.14/2019.
- Mafart P, Béliard E. 1994. *Ingeniería Industrial Alimentaria (Vol. II)*. Acribia, Zaragoza, Spain.
- Nierat TH, Musameh SM, Abdel-Raziq IR. 2013. Temperature and storage age (weekly basis)-dependence of olive oil viscosity. *MSAJ* **9** (11), 445–451.
- Sahasrabudhe SN, Rodriguez-Martinez V, O'Meara M, Farkas BE. 2017. Density, viscosity, and surface tension of five vegetable oils at elevated temperatures: Measurement and modeling. *Int. J. Food Prop.* **20** (sup2), 1965–1981. <https://doi.org/10.1080/10942912.2017.1360905>
- Singh PR, Heldman DR. 2009. *Introducción a la Ingeniería de los Alimentos*. Acribia, Zaragoza, Spain.
- Spiegel MR, Ribero OG. 1970. *Manual de fórmulas y tablas matemáticas*. McGraw-Hill, Mexico.
- Steffe JF. 1996. *Rheological methods in food process engineering*. Freeman press, East Lansing, MI, USA.
- Tirado, A. 2020. *Estudio de la densidad y la viscosidad de fluidos oleosos procedentes de almazara*. Trabajo Fin de Grado. ETSIAM - Universidad de Córdoba, Spain
- Uceda M, Jiménez A, Beltrán G. 2006. Trends in olive oil production. *Grasas Aceites* **57** (1), 25–31.
- Vallesquino P, Sánchez M. 2023. Un método para la determinación del contenido de agua de emulsiones de agua en aceite de oliva. *Actas del XXI Simposio Científico Técnico – Expoliva 2023 IND* – 1, 1–9.
- Vallesquino P, Tirado A. 2023. Un estudio sobre la densidad y la viscosidad de fluidos oleosos procedentes de almazara. *Actas del XXI Simposio Científico Técnico – Expoliva 2023 IND* – 8, 1–9.